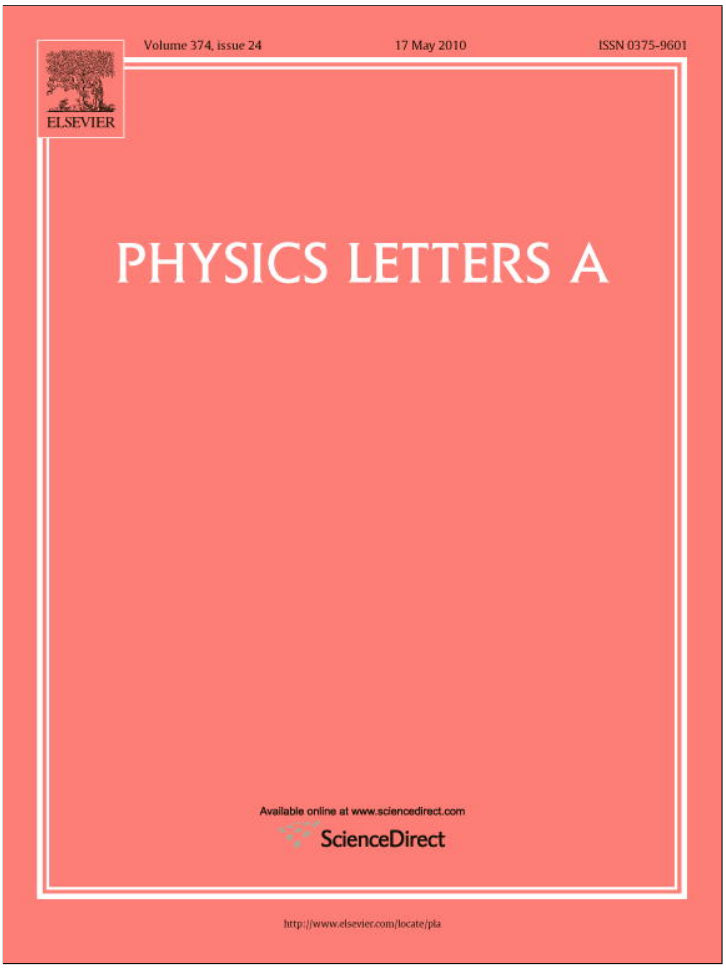

Physics Letters A 374 (2010) 2467–2474

Contents lists available at ScienceDirect

Physics Letters A

www.elsevier.com/locate/pla

Axisymmetric vibration of single-walled carbon nanotubes in water

C.Y. Wang *, C.F. Li, S. Adhikari

School of Engineering, Swansea University, Singleton Park, Swansea SA2 8PP, Wales, UK

ARTICLE INFO

Article history:
Received 13 January 2010
Received in revised form 31 March 2010
Accepted 1 April 2010
Available online 3 April 2010
Communicated by R. Wu

Keywords:
Single-walled carbon nanotubes
Water
Axisymmetric vibration
Van der Waals interaction

ABSTRACT

A double shell-Stokes flow model is developed to study the axisymmetric vibration of single-walled carbon nanotubes (SWCNTs) immerged in water. In contrast to macroscopic solid–liquid system, a submerged SWCNT is coupled with surrounding water via the van der Waals interaction. It is shown that this unique feature substantially reduces viscous damping of the axisymmetric radial, longitudinal and torsional vibrations and significantly up-shifts the frequency of the radial vibration of an SWCNT. The study offers a theoretical explanation for the experimental observation and molecular dynamics simulations available in particular cases, and provides an efficient modelling tool and useful guidance for the study of the general dynamic behaviour of SWCNTs in a fluid.

1. Introduction

Carbon nanotubes (CNTs) [1] have a broad range of potential applications in the next generation of nanotechnology, many of which will be implemented in a fluid environment. One of the typical examples is CNT-based nanofluidic devices [2] where fluid molecules are conveyed or stored inside nano-channels of CNTs. Such nanodevices can be used as chemical/biological sensors [3,4], cell/molecule transporters [5,6] and heat transporters [7]. The alternative interest lies in the use of CNTs submerged in a fluid, to name a few, CNT-based nanovehicles swimming in the human body to deliver drugs [8], nanorotors that use suspended CNTs [9] to stir up liquid in confined space and enhance diffusion process [8], and the CNT scanning probes for imaging in an aqueous environment [10]. Obviously, an in-depth understanding of the CNT–fluid interaction and its effect on the mechanical behaviour of CNTs are essential to the development of the CNT-based nanodevices running in the presence of a fluid phase.

Up till now, considerable effort has been made to study the dynamic and static behaviour of the fluid inside CNTs [2,11] and its influence on the vibration and buckling of CNTs [12–17]. Nevertheless, only one particular vibration mode, i.e., the radial breathing (RB) vibration was studied [18–20] for CNTs immersed in a fluid. It is shown that the fluid significantly raises the RB frequency [18,20] rather than extinguishing the vibration *via* the viscous damping. This unintuitive result infers that in the presence of fluids CNTs can still serve as Terahertz resonators in NanoElectroMechincal System. On the other hand, the vibration could also exert strong impact on the mechanical integrity of CNTs and in turn, significantly affect the proper functioning of CNT-based nanodevices in an aqueous environment. Recently, Longhurt and Quirke [21–23] further studied the RB vibration for single-walled CNTs (SWCNTs) in water using multi-scale modelling. In their molecular dynamic (MD) simulation the authors observed a layer of water molecules absorbed on the surface of SWCNTs. In particular, the van der Waals (vdW) interaction between the absorbed water and the SWCNTs is found to be responsible for the up-shift of the RB frequency in a fluid [21–23]. This milestone study has paved the way for an investigation on the general vibration behaviour of SWCNTs in a fluid, which still remains an open topic in nanomechanics. Evidently, such a study necessitates a suitable model for SWCNTs, the SWCNT–water interaction and the water flow in the surrounding area.

Various mechanical models for CNTs have been used in the literature. Such models include, but are not limited to Euler beam model [24] and more involved structural mechanics model [25–27]. Specifically, the elastic shell model was efficiently used for the mechanical behaviour of CNTs [28–31] and microtubules (MTs) in eukaryotic cells [32–35] with good agreement with experiments [33] and atomistic simulations [29,31]. In addition, the dimensional analysis [35] showed that the fluid motion surrounding nanoscale tubes can be considered as the Stokes flow with a Reynolds number much smaller than unity [36]. Motivated by these earlier studies, we have developed a double shell-Stokes flow model for the single-walled CNT (SWCNT)–water coupling system. Here the core SWCNT and the absorbed layer of water

* Corresponding author.
E-mail address: chengyuan.wang@swansea.ac.uk (C.Y. Wang).

0375-9601/$ – see front matter
doi:10.1016/j.physleta.2010.04.002

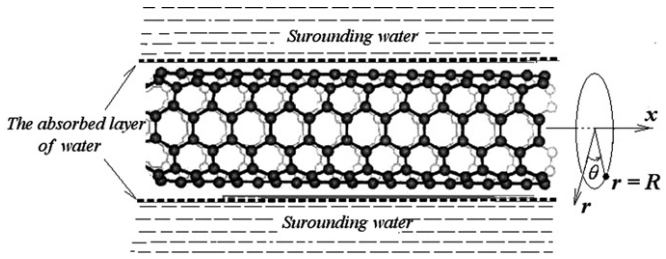

Fig. 1. The schematic diagram of the SWCNT–water coupling system.

are modelled as two-layer thin shells coupled via the interlayer vdW interaction. The external water is modelled as the Stokes-flow. Based on the model we study the axisymmetric vibration of SWCNTs in water, i.e., axisymmetric radial, longitudinal and tangential modes, which can be used as probes for the geometric size [18], the atomistic structures [19] and the material properties [37] of SWCNTs and thus, are of major engineering and scientific interest.

2. The double shell-Stokes flow model

This Letter aims to study the axisymmetric vibration of SWCNTs submerged in water. In doing this we shall first develop an appropriate model for the solid–fluid coupling system at nanoscale, which is substantially different from their macroscopic counterpart. As shown in Fig. 1, this system comprises three constituent parts, i.e., the inner (sealed) SWCNT, the absorbed layer of water molecules [21–23] and the water flow surrounding the absorbed layer. The core SWCNT is coupled with the absorbed layer of water through the normal interlayer vdW interaction [21–23].

2.1. Double shell model for the SWCNT–absorbed water system

SWCNTs are one-atom layer cylindrical shells where carbon atoms are connected via chemical bonds in hexagonal arrangement. Such discrete shells deform through the changes of the in-plane σ-bond and off-plane π-bond of carbon atoms, which contrasts with the deformation mechanisms of 3D continuum thin shells [31]. Thus, as shown in [31], SWCNTs may not have a well defined effective wall-thickness and equivalent Young's modulus [31,38,39]. On the other hand, the continuum 2D constitutive relations still hold true for SWCNTs [38], i.e., the equivalent strains are related to the membrane forces via in-plane extension stiffness (K), in-plane torsional stiffness, bending stiffness (D) and off-plane torsional stiffness. Specifically, the values of these stiffnesses can be measured directly in atomistic simulations without defining the effective wall thickness and Young's modulus. It is thus more realistic to model SWCNTs as 2D elastic shells with the above four stiffnesses as material constants [31]. Based on this model [31], the dynamic equations are derived for the axisymmetric vibration of SWCNTs (Appendix A):

$$K\cdot\left(r_{cnt}^2\frac{\partial^2 u}{\partial x^2}-r_{cnt}\nu\frac{\partial w}{\partial x}\right)+D\cdot\left(r_{cnt}\frac{\partial^3 w}{\partial x^3}\right)=\rho\cdot r_{cnt}^2\frac{\partial^2 u}{\partial t^2}, \tag{1a}$$

$$K\cdot\left(\frac{r_{cnt}^2(1-\nu)}{2}\cdot\frac{\partial^2 v}{\partial x^2}\right)+D\cdot\left(\frac{3(1-\nu)}{2}\cdot\frac{\partial^2 v}{\partial x^2}\right)=\rho\cdot r_{cnt}^2\frac{\partial^2 v}{\partial t^2}, \tag{1b}$$

$$K\cdot\left(r_{cnt}\nu\frac{\partial u}{\partial x}-w\right)-D\cdot\left(r_{cnt}^2\frac{\partial^4 w}{\partial x^4}+r_{cnt}\frac{\partial^3 u}{\partial x^3}+\frac{w}{r_{cnt}^2}\right)=r_{cnt}^2\cdot\left(\rho\cdot\frac{\partial^2 w}{\partial t^2}-p_{cnt}\right). \tag{1c}$$

Here x and θ are the axial and angular circumferential coordinates; u, v and w are the axial, circumferential and (inward positive) radial displacements, respectively; r_{cnt} is the radius, ρ is the mass density per unit area and ν is the Poisson ratio of an SWCNT; t is the time and p_{cnt} is the (inward positive) radial pressure on the core SWCNT due to its normal vdW interaction with the absorbed layer of water molecules.

Similar to Ref. [23], the absorbed layer of water will be treated as a flexible membrane shell whose four elastic stiffnesses vanish and its rigidity is solely represented by the CNT–water surface tension (γ) on the absorbed layer of water, i.e., a constant membrane tensile force that is identical in all directions. This is equivalent to the stress state of a membrane subject to initial axial and circumferential tensile forces of the same magnitude γ. In the equilibrium state, there is a net force of zero inside the water shell whereas, during the axisymmetric vibration, the surface tension (γ) generates nonzero net forces (per unit area) $\gamma\cdot(\frac{\partial w_w}{r_w\partial x}+\frac{\partial^2 u_w}{\partial x^2})$, $\gamma\cdot(\frac{\partial^2 v_w}{\partial x^2})$ and $-\gamma\cdot(\frac{\partial u_w}{r_w\partial x})+\gamma\cdot\frac{\partial^2 w_w}{\partial x^2}$ in x, θ and radial (r) directions, respectively [40], where u_w, v_w and w_w are the displacements in the three directions, and r_w is the radius of the water shell. The equations for the axisymmetric vibration of the water shell can then be obtained as

$$\begin{aligned}
&\gamma\cdot\left(\frac{\partial w_w}{r_w\partial x}+\frac{\partial^2 u_w}{\partial x^2}\right)+P_{rx}=\rho_w\cdot\frac{\partial^2 u_w}{\partial t^2},\\
&\gamma\cdot\left(\frac{\partial^2 v_w}{\partial x^2}\right)+P_{r\theta}=\rho_w\frac{\partial^2 v_w}{\partial t^2},\\
&-\gamma\cdot\left(\frac{\partial u_w}{r_w\partial x}\right)+\gamma\cdot\frac{\partial^2 w_w}{\partial x^2}-p_w+P_{rr}=\rho_w\frac{\partial^2 w_w}{\partial t^2}.
\end{aligned} \tag{2}$$

Here ρ_w is the mass density per unit area of the water shell; p_w is the (inward positive) radial pressure on the inner surface of the water shell due to the vdW interaction and P_{rx}, $P_{r\theta}$ and P_{rr} are the axial, circumferential and radial stresses on the outer surface of the water shell due to surrounding water. The vdW interaction p_{cnt} and p_w are action and reaction, which can be calculated by [21–23,28–30].

$$p_{cnt} = c \cdot (w_w - w) \quad \text{and} \quad p_w = -\frac{r_{cnt}}{r_w} \cdot p_{cnt} \tag{3}$$

where c is the vdW interaction coefficient defined as the second derivative of the interlayer potential with respect to interlayer spacing. Such a linear model has been widely used for the interlayer vdW interaction in multi-walled CNTs (MWCNTs) [29,30] and those between CNTs and water [21–23] with excellent agreement with MD simulations [21–23,29]. Since SWCNTs are usually of a large length-to-diameter aspect ratio, we shall treat SWCNTs and the external water shell as infinitely long shells. The solution of Eqs. (1) and (2) can be assumed as [35]

$$\begin{bmatrix} u \\ v \\ w \end{bmatrix} = \begin{bmatrix} U \\ V \\ -iW \end{bmatrix} \exp(ik_x x - i\omega t) \quad \text{and} \quad \begin{bmatrix} u_w \\ v_w \\ w_w \end{bmatrix} = \begin{bmatrix} U_w \\ V_w \\ -iW_w \end{bmatrix} \exp(ik_x x - i\omega t) \tag{4}$$

where (U, V, W) and (U_w, V_w, W_w) represent the initial vibration amplitudes (at $t = 0$) of SWCNTs and the water shell in axial, circumferential and radial directions, respectively. k_x is the wave vector (nm^{-1}) in the axial direction. The real part of ω ($\text{Re}(\omega)$) gives the angular frequency that is related to the frequency by $f = \frac{\text{Re}(\omega)}{2\pi}$. In addition, as seen in Eq. (4), the vibration amplitude at time $t = T > 0$ can be calculated by the initial vibration amplitude times $e^{\text{Im}(\omega)\cdot T}$, where $\text{Im}(\omega)$ is the imaginary part of ω. Thus, when $\text{Im}(\omega) < 0$, the vibration decays exponentially with the time. In other words, the negative $\text{Im}(\omega)$ measures the damping of the associated vibration modes.

2.2. Stokes-flow model for the surrounding water

In Fig. 1, the water shell is surrounded by the exterior water which will be flowing due to the water shell oscillation induced by the vibration of the core SWCNT. The motion of the water could exert influence on the vibration of the SWCNT but was not considered in previous studies [21–23]. A suitable model of the water flow is crucial for a reliable description to the vibration of an SWCNT in water. To develop this model, we shall first conduct a dimensional analysis to estimate the Reynolds number of the water flow induced by SWCNT vibration. Here let us consider the RB vibration, a special axisymmetric radial mode that has been observed experimentally for SWCNTs in a fluid [18–20]. It was shown [23] that the RB frequency in water is of the order of 229 cm^{-1} for SWCNTs with radius (r) around 0.5 nm. This frequency corresponds to the RB vibration mainly of the core SWCNT whose vibration amplitude is at least an order of magnitude larger than that of the outer water shell [23]. Assuming that the vibration amplitude of SWCNT is 0.1 nm (i.e., 10 times smaller than its diameter), the vibration amplitude (A) of the water shell should be of the order of 0.01 nm. The average velocity of the water flow adjoining the water shell can then be estimated as $v \leqslant 4 \cdot A \cdot f_{RB} \approx 1.4 \times 10^3$ m/s. Accordingly, the Reynolds number of the water flow, calculated by $Re = \frac{\rho_{water} \cdot v \cdot r_{cnt}}{\mu_w}$, is of the order of 0.1 or even smaller ($\rho_{water} = 1000$ kg/m^3 and $\eta = 1.003 \times 10^{-3}$ N s/m^2 [36] are the mass density and dynamic viscosity of water (20 °C)). The water flow can thus be modelled as the Stokes flow whose governing equations are as follows when its gravity is ignored [36]

$$\nabla \bullet \tilde{v} = 0 \quad \text{and} \quad \nabla p = \eta \cdot \nabla^2 \tilde{v}. \tag{5}$$

Here $\tilde{v}$ is the velocity of the water flow with three components $\tilde{v}_x$, $\tilde{v}_\theta$ and $\tilde{v}_r$ in radial, circumferential and axial directions and p is the pressure in water. On the surface of the water shell (i.e., $r = r_w$), the continuity condition requires that the water flow moves at the same velocity as that of the water shell, i.e.,

$$\tilde{v}_x|_{r=r_w} = \left.\frac{\partial u_w}{\partial t}\right|_{r=r_w}, \qquad \tilde{v}_\theta|_{r=r_w} = \left.\frac{\partial v_w}{\partial t}\right|_{r=r_w} \quad \text{and} \quad \tilde{v}_r|_{r=r_w} = \left.\frac{\partial w_w}{\partial t}\right|_{r=r_w}. \tag{6}$$

By using Eqs. (4)–(6), the stresses acting on the outer surface of the water shell due to the surrounding water flow can be obtained as

$$\begin{bmatrix} P_{rx} \\ P_{r\theta} \\ P_{rr} \end{bmatrix} = \begin{bmatrix} A_{rx} \\ A_{r\theta} \\ A_{rr} \end{bmatrix} \cdot \frac{\eta \cdot \omega \cdot \exp(ik_x x - i\omega t)}{r_w}. \tag{7}$$

The derivation of Eq. (7) and the form of A_{rx}, $A_{r\theta}$ and A_{rr} can be found in Appendix B.

2.3. Vibration analysis of the SWCNT–water system

By substituting Eqs. (3), (4) and (7) into Eqs. (1) and (2), the original partial differential equation can be transformed into a set of algebraic equations as

$$H(k, \omega)_{6\times 6} \cdot [U, V, W, U_w, V_w, W_w]^T = 0 \tag{8}$$

where H is a 6×6 matrix. The existence condition of a nonzero solution of (U, V, W) and (U_w, V_w, W_w) is:

$$\det H(k, \omega)_{6\times 6} = 0. \tag{9}$$

Solving Eq. (9) gives the eigenvalue ω whose real part is the vibration frequency of the SWCNT–water system. Substituting the obtained value of ω into Eq. (8), one can calculate the amplitude ratios ($\frac{U}{W}$, $\frac{V}{W}$, 1, $\frac{U_w}{W}$, $\frac{V_w}{W}$, $\frac{W_w}{W}$) defining the vibration mode associated with the frequency.

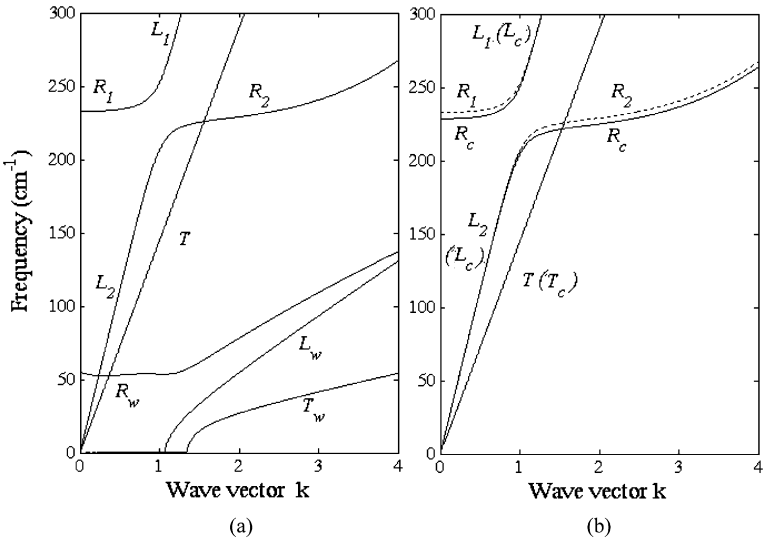

Fig. 2. The frequency of the axisymmetric vibration is obtained in (a) for an SWCNT–water system, where R_1 (R_2), L_1 (L_2) and T represent axisymmetric radial, longitudinal and torsional vibration primarily of the SWCNT, and R_w, L_w and T_w denote those mainly of the water shell. R_1 (R_2), L_1 (L_2) and T (dotted lines in (b)) of the submerged SWCNT are compared with their counterparts of the free SWCNT, i.e., R_c, L_c and T_c, in (b).

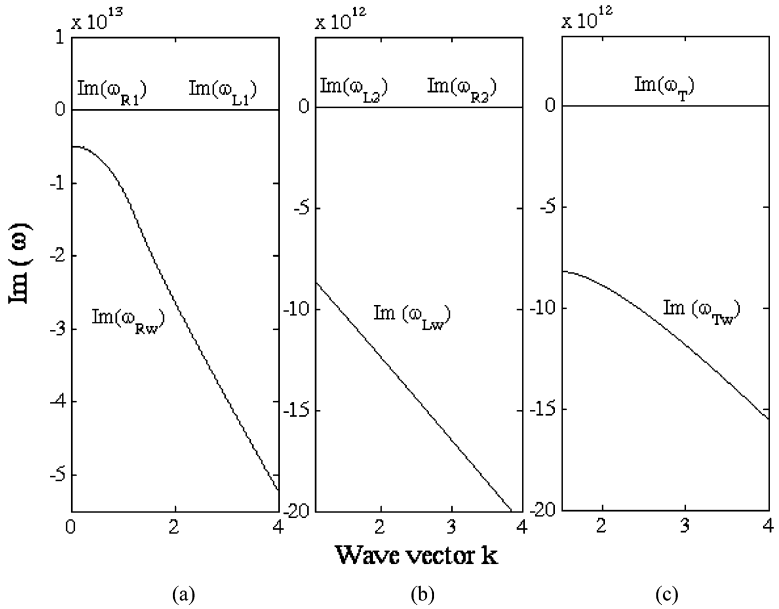

Fig. 3. The imaginary part of ω, i.e., Im(ω), corresponding to the vibration curves shown in Fig. 2(a). (a) Im(ω_{R_1}) and Im(ω_{L_1}) associated with of R_1 and L_1, and Im(ω_{R_w}) associated with R_w, (b) Im(ω_{L_2}) and Im(ω_{R_2}) associated with of L_2 and R_2, and Im(ω_{R_w}) associated with R_w, and (c) Im(ω_T) and Im(ω_{T_w}) associated with T and T_w, respectively.

3. Results and discussion

In this section, the axisymmetric vibration will be investigated for SWCNTs immerged in water. To this end SWCNTs with a typical diameter 1.03 nm will be used as an example. The values of material constants are $K = 360$ J/nm, $D = 2$ eV, $\rho = (2.27\ \text{g/cm}^3) \times 0.34$ nm and $\nu = 0.2$ for SWCNTs [28,31]. In addition, the values of ρ_w and γ of the water shell and the vdW interaction coefficient c between the SWCNT and water shell can be extracted by fitting the double shell model to the MD simulations [21–23] for the radial breathing mode (i.e., the axisymmetric radial vibration with $k_x = 0$) with zero external pressure. The interlayer spacing (s) between the core SWCNTs and the water shell can be obtained directly in Refs. [21,22]. The radius of water shell r_w can then be obtained by $r_w = r_{cnt} + s$.

Following the procedure in Section 2, the phonon dispersion relations are obtained in Fig. 2(a) for the core SWCNT and the concentric water shell around it. In particular, the dispersion curves of the SWCNT in the presence of water (dotted line) are compared in Fig. 2(b) with their counterparts in the absence of water (solid lines). In Fig. 2(a), six frequency curves are obtained for the SWCNT–water shell system and labelled with the corresponding vibration modes, e.g., the radial (R), longitudinal (L) and torsional (T) modes. Here the notations with subscript w denote the vibration mainly of the water shell while others represent those primarily of the core SWCNT. It is noted in Fig. 2(a) that for different values of $k(= r_{cnt}k_x)$ the same frequency curve could correspond to different vibration modes. The imaginary part of ω (i.e., Im(ω)) associated with the frequencies in Fig. 2(a) (i.e., Re(ω)/2π) are presented in Fig. 3 measuring the viscous damping of the corresponding vibrations.

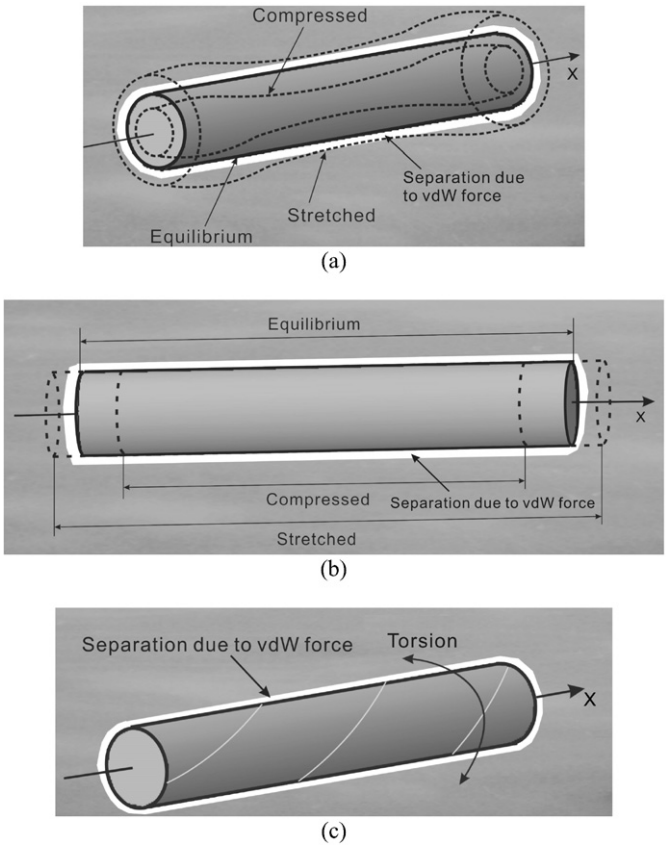

Fig. 4. Illustration of axisymmetric vibration of an SWCNT, i.e., (a) axisymmetric radial vibration, (b) axisymmetric longitudinal vibration, and (c) axisymmetric torsional vibration.

3.1. Axisymmetric radial vibration

Let us first look at the R mode (i.e., R_1 and R_2) in Fig. 2(a), which represents the axisymmetric radial vibration mainly of the submerged SWCNT. As illustrated in Fig. 4(a) for the axisymmetric R mode, the predominant radial displacement of the SWCNT (as a function of time) does not change along the circumferential direction but varies periodically in the axial direction with an axial wavelength of $\lambda = \frac{2\pi \cdot r_{cnt}}{k}$. It is seen from Fig. 2(a) that the frequency of such R modes decreases monotonically with decreasing k, i.e., increasing axial wavelength λ. It approaches an asymptotic value of 229 cm^{-1} when k becomes sufficiently small, i.e., axial wavelength λ is long enough. In particular, at $k = 0$, i.e., infinitely long axial wavelength λ, R mode turns into RB mode of SWCNTs where the radial vibration is uniform along both axial and circumferential directions as if the whole tube was breathing. The analysis of the amplitude ratios ($\frac{U}{W}$, $\frac{V}{W}$, 1, $\frac{U_w}{W}$, $\frac{V_w}{W}$, $\frac{W_w}{W}$) further indicates that, in this R mode, the vibration of the water shell and the resulting water flow surrounding the water shell are negligible as compared with the radial vibration of the SWCNT. In other words, the exterior water is virtually at rest when the submerged SWCNT is vibrating in radial direction, i.e., the water neighbouring the SWCNT behaves simply like an equivalent rigid body. This observation based on the present model can be explained by the fact that the core SWCNT is not directly in touch with the water shell but coupled with it via the interlayer vdW interaction. Such SWCNT–water coupling is not strong enough as compared with the equivalent radial rigidity of the water shell that originates from the surface tension of the absorbed water layer and the strengthening effect on the water shell given by the exterior water. As a result, the radial motion cannot be efficiently transferred from the inner SWCNT to the external water. This result given by the present model justifies the rigid-shell assumption for the absorbed water layer in studying RB mode of SWCNTs in water [21,22]. Specifically, in this case, the energy dissipation due to the predominant effect of the friction in the Stokes flow (i.e., the flow of surrounding water) can be reasonably neglected. Ideally, the energy of such a vibration system is nearly conserved, which would lead to negligible damping of the radial vibration of the SWCNTs immerged in water. Consistent with these analyses, our numerical results in Fig. 3 reveal that the imaginary part of ω associated with the R mode (i.e., $\text{Im}(\omega_{R_1})$ in Fig. 3(a) and $\text{Im}(\omega_{R_2})$ in Fig. 3(b)) almost vanishes, showing that the vibration amplitude of the SWCNT remains almost constant independent of time. It then follows that in the presence of water SWCNTs can vibrate almost freely in radial direction. Here the negligible damping of the vibration is a result of the interlayer vdW interaction between the core SWCNT and the absorbed water molecules.

Furthermore, the comparison made in Fig. 2(b) demonstrates that the radial vibration of the SWCNT in water exhibit frequency 233 cm^{-1} (dotted lines), which is more than 4 cm^{-1} higher than its counterpart in the absence of water (solid lines). The up-shift of the frequency can again be attributed to the interlayer vdW interaction between the SWCNT and the surrounding water. Such a phenomenon was observed previously for radial breathing mode at $k = 0$ [21–23]. In particular, the present study shows that the up-shift of the R mode frequency remains almost a constant throughout the whole length of k considered here. This suggests that the effect of the vdW interaction on the R mode frequency is independent of the axial wavelength of the radial vibration. Here it is noted that the above obtained effects of exterior water on the axisymmetric R mode of SWCNTs are found to be in agreement with existing experimental observation [18,20] and MD simulations [21–23] available for RB mode of SWCNTs, i.e., the axisymmetric R mode with $k = 0$ or an infinite

axial wavelength. In these previous studies, the up-shift of 2 to 10 cm^{-1} is obtained for the RB mode of SWCNTs in a fluid whereas no viscous damping has ever been reported.

As shown before, these unique features of the radial vibration in water are due to the interlayer vdW interaction, which is a result of the large surface-to-volume ratio of the nanoscale SWCNTs. Indeed, this character distinguishes such a nanoscale solid–fluid coupling system from its macroscopic counterpart where the surrounding fluid is in contact with the solid and thus, moves with the solid at the same speed on the solid–fluid interface. Consequently, the strong damping would occur for the radial vibration of the macroscopic solid–fluid system.

In Fig. 2(a), another vibration mode R_w with significant radial displacement is obtained at a low frequency around 56 cm^{-1} when k increases from zero to one. In this mode, the radial displacement of water shell is comparable with its axial displacement but greater than its circumferential displacement and all displacements of the core SWCNT. In the SWCNT–water system the surrounding water is moving with the absorbed layer (i.e., the water shell) at the interface with exactly the same velocity (see boundary condition (6)). Thus, in this R_w mode, significant motion of exterior water will be generated in the neighbourhood of the water shell. Naturally, the friction of the water flow as the Stokes flow will lead to the substantial energy dissipation of the R_w mode. Consequently, as shown in Fig. 3(a) the imaginary part of ω associated with R_w, i.e., $\mathrm{Im}(\omega_{R_w})$, is a negative real number whose absolute value is of the order of magnitude 10^{13}. These results indicate that due to the viscous damping effect of the Stokes flow, the vibration amplitude of the R_w mode will decrease drastically with time, i.e., the excitation of the R_w mode will be quenched by the surrounding water in a very short period. For example, suppose $\mathrm{Im}(\omega_{R_w}) = -10^{13}$ the half life of the R_w mode is only 0.07 pico-second. It is thus concluded that, in reality, R_w mode cannot exist in the SWCNT–water system. This explains the reason as to why such a low frequency R mode with substantial vibration of the water shell has never been observed in experiments as discussed in Ref. [23].

3.2. Axisymmetric longitudinal and torsional vibration

Next we shall study the axisymmetric L and T modes of the SWCNT–water system. In doing this let us first consider the longitudinal vibration of the submerged SWCNT, i.e., L_1 and L_2 modes in Fig. 2(a), where, as shown in Fig. 4(b), the SWCNT is stretching or shrinking with time along the axial direction. Here it is noted in Eqs. (1a) and (1c) that the longitudinal vibration of an SWCNT is generally coupled with its radial vibration primarily due to the Poisson ratio effect. This coupling effect is very strong in the transition zone between R_1 and L_1 modes, and L_2 and R_2 modes (Fig. 2(a)) where the radial displacement is comparable with the longitudinal one. However, such coupling becomes much less pronounced for the L_1 and L_2 modes where the longitudinal displacement is orders of magnitudes greater than the radial one. Accordingly, in the L mode of the SWCNT, the SWCNT–water shell coupling via the normal vdW interaction is very weak and can almost be neglected in vibration analysis. This character results in two consequences: firstly as we can see from Fig. 2(b), the longitudinal vibrations of the submerged SWCNTs have almost the identical frequency to their counterparts of the individual SWCNT showing negligible effect of the vdW interaction on L mode frequency. Secondly, due to the separation between the SWCNT and the exterior water, the surrounding water (including the water shell) is nearly at a stationary state and the energy loss of the vibration caused by the friction of the water flow can be safely neglected. Thus, analogous to the case of the radial vibration (Section 3.1), in Figs. 3(a) and 3(b) the imaginary part of ω associated with L modes, i.e., $\mathrm{Im}(\omega_{L_1})$ and $\mathrm{Im}(\omega_{L_2})$, is almost zero. These results reveal that the longitudinal vibration of an SWCNT will not decay with time even when the SWCNT is submerged in water.

For the torsional vibration illustrated in Fig. 4(c), it is seen from Eq. (1b) that the circumferential displacement of an SWCNT is decoupled with its longitudinal and radial displacements. Thus, the interlayer vdW interaction in the radial direction has absolutely no effect on the axisymmetric torsional vibration of the SWCNT. Naturally, such a torsional vibration of the SWCNT is independent of the surrounding water. As a result, the T mode frequency of the submerged SWCNT coincides with its counterpart of the isolated SWCNT in Fig. 2(b). In addition, the imaginary part of ω associated with the T mode (i.e., $\mathrm{Im}(\omega_T)$) goes to zero in Fig. 3(c). This means that, in the presence of water the axisymmetric torsional vibration of the SWCNT is an undamped free vibration completely decoupled with the motion of surrounding water. Here it is emphasized that similar to the case of radial vibration, the unique features of longitudinal and torsional vibrations again arise from the vdW interaction between the SWCNT and the absorbed layer of water.

In Fig. 2(a), L_w and T_w are also obtained for the SWCNT–water system, which represent the vibration mainly of the water shell. Here, L_w denotes the vibration modes of the water shell with its longitudinal displacement comparable with the radial one but orders of magnitude larger than the circumferential displacements. T_w denotes the vibration with a substantial circumferential displacement. The continuity condition (6) on the interface of the water shell and the surrounding water requires that, at the interface the surrounding water moves with the water shell at the same speed. Thus, L_w and T_w modes will induce the flow of the surrounding water and then, the damping of the vibration due to the dominant effect of friction in the surrounding Stokes flow. Thus in Figs. 3(b) and 3(c) we have negative imaginary parts of ωassociated with L_w and T_w modes, i.e., $\mathrm{Im}(\omega_{L_w})$ and $\mathrm{Im}(\omega_{T_w})$. Here it is noted in Fig. 3 that absolute values of $\mathrm{Im}(\omega_{L_w})$ and $\mathrm{Im}(\omega_{T_w})$, i.e., the damping of the vibration, increases rapidly with increasing k and rising frequency. In Fig. 2(a), when $k = 2$ the L_w and T_w mode frequencies are approximately 55 and 27 cm^{-1}, respectively, and the corresponding $\mathrm{Im}(\omega_{L_w})$ and $\mathrm{Im}(\omega_{T_w})$ shown in Figs. 3(b) and 3(c) are of the order of -10^{13}. Based on these data the release time τ-to-period $(1/f)$ ratios calculated for L_w and T_w modes are much less than unit, which suggests that these water-shell vibrations will be extinguished right after their excitation. Furthermore, in the range of small k, e.g., $k < 1$ the frequency becomes zero in Fig. 2(a) and $\mathrm{Im}(\omega_{L_w})$ and $\mathrm{Im}(\omega_{T_w})$ obtained in our calculation are still negative. In this case, L_w and T_w modes correspond to the non-oscillating motions of the SWCNT–water system. These vibration modes obviously cannot be detected in real cases and thus cannot exert significant influence on the mechanical behaviour of the core SWCNTs.

4. Conclusion

The double shell-Stokes flow model has been developed for the dynamical behaviour of an SWCNT–fluid system and utilized to study the axisymmetric vibration of SWCNTs in water. An SWCNT is a nanoscale cylindrical shell, which exhibits a large surface-to-volume ratio and significant vdW interaction with the surrounding fluid. It is this unique feature that distinguishes the SWCNT–water system from

its macroscopic counterparts and gives rise to the distinctive vibrational behaviour of a submerged SWCNT. The present study aims to examine the effect of the CNT–fluid coupling on the vibration of SWCNTs. The new findings are summarised as follows.

1. For SWCNTs immerged in water, the vdW interaction between the SWCNTs and surrounding water significantly raises the frequency of the axisymmetric radial modes, but has negligible effect on that of the axisymmetric longitudinal mode and absolutely no influence on that of the axisymmetric torsional mode.
2. The vdW interaction separates the submerged SWCNTs from the exterior water, which efficiently prevent the vibration of the SWCNT from being transferred to the surrounding water and in turn, substantially reduces viscous damping effect of water. As a result, damping of the axisymmetric vibrations is negligible for SWCNTs in water.
3. On the other hand, the excitation of the vibration primarily of the water molecules absorbed on the submerged SWCNTs will be extinguished very quickly due to the strong viscous damping of the exterior water.
4. It is thus concluded that, in the water–SWCNT system, surrounding water basically behaves like a rigid body interacting with the vibrating SWCNT via the vdW interaction. This equivalent model accounts for the aforementioned unique features of axisymmetric vibration in water and provide guidance to future study of the general vibration behaviour of CNTs in an aqueous environment.

Appendix A

The governing equations for free vibration of an SWCNT subject to a uniform radial pressure can be obtained base on Flugge shell theory [29,30].

$$
\begin{aligned}
&r_{cnt}^2\frac{\partial^2 u}{\partial x^2}+\frac{1}{2}(1-\nu)\frac{\partial^2 u}{\partial\theta^2}+\frac{r_{cnt}}{2}(1+\nu)\frac{\partial^2 v}{\partial x\partial\theta}-\nu r_{cnt}\frac{\partial w}{\partial x}+\frac{D}{K\cdot r_{cnt}^2}\cdot\left[\frac{1}{2}(1-\nu)\frac{\partial^2 u}{\partial\theta^2}+r_{cnt}^3\frac{\partial^3 w}{\partial x^3}-\frac{r_{cnt}}{2}(1-\nu)\frac{\partial^3 w}{\partial x\partial\theta^2}\right]\\
&\quad=\frac{\rho}{K}\cdot r_{cnt}^2\frac{\partial^2 u}{\partial t^2},\\
&\frac{r_{cnt}}{2}(1+\nu)\frac{\partial^2 u}{\partial x\partial\theta}+\frac{r_{cnt}^2}{2}(1-\nu)\frac{\partial^2 v}{\partial x^2}+\frac{\partial^2 v}{\partial\theta^2}-\frac{\partial w}{\partial\theta}+\frac{D}{K\cdot r_{cnt}^2}\cdot\left[\frac{3r_{cnt}^2}{2}(1-\nu)\frac{\partial^2 v}{\partial x^2}+\frac{r_{cnt}^2}{2}(3-\nu)\frac{\partial^3 w}{\partial x^2\partial\theta}\right]=\frac{\rho}{K}\cdot r_{cnt}^2\frac{\partial^2 v}{\partial t^2},\\
&\nu r_{cnt}\frac{\partial u}{\partial x}+\frac{\partial v}{\partial\theta}-w+\frac{D}{K\cdot r_{cnt}^2}\cdot\left[-r_{cnt}^3\frac{\partial^3 u}{\partial x^3}+\frac{r_{cnt}}{2}(1-\nu)\frac{\partial^3 u}{\partial x\partial\theta^2}-\frac{r_{cnt}^2}{2}(3-\nu)\frac{\partial^3 v}{\partial x^2\partial\theta}-r_{cnt}^4\cdot\nabla^4 w-w-2\frac{\partial^2 w}{\partial\theta^2}\right]\\
&\quad=\frac{1}{K}\cdot r_{cnt}^2\cdot\left(\rho\frac{\partial^2 w}{\partial t^2}-p_{cnt}\right).
\end{aligned}
\tag{A.1}
$$

For axisymmetric vibration we have $\frac{\partial}{\partial\theta}=0$. Substituting this condition into (A.1) leads to the governing equations for axisymmetric vibration of an SWCNT subject to a uniform radial pressure p_{cnt}, i.e., Eq. (1) in text.

Appendix B

The Stokes-flow satisfies Eq. (5) when its gravity is ignored. The general solution of Eq. (5) in the cylindrical coordinates (r,θ,x) is [36]:

$$
\begin{cases}
\tilde{v}_r=r\frac{\partial}{\partial r}(\frac{\partial\Pi}{\partial r})+\frac{\partial\Psi}{\partial r}+\frac{\partial\Omega}{r\partial\theta},\\
\tilde{v}_\theta=r\frac{\partial}{\partial r}(\frac{1}{r}\frac{\partial\Pi}{\partial\theta})+\frac{\partial\Psi}{r\partial\theta}-\frac{\partial\Omega}{\partial r},\\
\tilde{v}_x=r\frac{\partial}{\partial r}(\frac{\partial\Pi}{\partial x})+\frac{\partial\Pi}{\partial x}+\frac{\partial\Psi}{\partial x},\\
p=-2\mu\frac{\partial^2\Pi}{\partial x^2}
\end{cases}
\tag{B.1}
$$

where Π, Ψ, Ω are potential functions satisfying Laplace's equation

$$
\begin{cases}
\nabla^2\Pi=0,\\
\nabla^2\Psi=0,\\
\nabla^2\Omega=0.
\end{cases}
\tag{B.2}
$$

On the outer surface of the water shell $r=r_w$, the boundary condition of water surrounding the water shell is specified by Eq. (6), where

$$
\begin{cases}
\frac{\partial u_w}{\partial t}=-iU_w\omega\exp(ik_x x-i\omega t),\\
\frac{\partial v_w}{\partial t}=-iV_w\omega\exp(ik_x x-i\omega t),\\
\frac{\partial w_w}{\partial t}=-W_w\omega\exp(ik_x x-i\omega t).
\end{cases}
\tag{B.3}
$$

Provided that the fluid velocity at the infinity is finite, the general solution of (B.2) can be expressed as the superposition of a sequence of harmonic functions, each of which is of the following form [36]

$$
\begin{cases}
\Pi=C_\Pi K_n(k_x r)\exp(in\varphi+ik_x x),\\
\Psi=C_\Psi K_n(k_x r)\exp(in\varphi+ik_x x),\\
\Omega=C_\Omega K_n(k_x r)\exp(in\varphi+ik_x x)
\end{cases}
\tag{B.4}
$$

where C_Π, C_Ψ, C_Ω are constants, and $K_n(k_x r)$ is the modified Bessel function of the second kind. In particular, for the axisymmetric vibration of the SWCNT–water system the value of integer n is zero. Substituting (B.4) into (B.1) and utilizing the boundary condition (6) on the water shell surface $r=r_w$. The constants C_Π, C_Ψ, C_Ω can be expressed with U_w, V_w, W_w, ω, and k_x

$$C_{\Pi} = \frac{r_w \cdot \omega \exp(-i\omega t)(U_w k K_1^2 + W_w k \cdot K_0 K_1)}{k \cdot (k^2 K_1^3 - 2k \cdot K_0 K_1^2 - k^2 K_0^2 K_1)},$$
$$C_{\Psi} = \frac{r_w \cdot \omega \exp(-i\omega t)((W_w k + U_w) k K_1^2 + (U_w k^2 - W_w k) K_0 K_1)}{k \cdot (k^2 K_1^3 - 2k \cdot K_0 K_1^2 - k^2 K_0^2 K_1)},$$
$$C_{\Omega} = \frac{i\omega \exp(-i\omega t)(-V_w k^2 K_1^2 + 2V_w k \cdot K_0 K_1 + V_w k^2 \cdot K_0^2)}{k \cdot (k^2 K_1^3 - 2k \cdot K_0 K_1^2 - k^2 \cdot K_0^2 K_1)} \tag{B.5}$$

where $k = k_x r_w$, $K_0 = K_0(k)$ and $K_1 = K_1(k)$.

In the cylindrical coordinate system, the normal stress P_{rr}, the shear stresses $P_{r\theta}$ and P_{xr} are given by

$$\begin{cases} P_{rr} = -p + 2\mu_w \frac{\partial \tilde{v}_r}{\partial r}, \\ P_{r\theta} = \mu_w (\frac{1}{r}\frac{\partial \tilde{v}_r}{\partial \theta} + \frac{\partial \tilde{v}_\theta}{\partial r} - \frac{\tilde{v}_\theta}{r}), \\ P_{xr} = \mu_w (\frac{\partial \tilde{v}_x}{\partial r} + \frac{\partial \tilde{v}_r}{\partial x}). \end{cases} \tag{B.6}$$

Substituting (B.1) into (B.6) and replacing Π, Ψ, Ω and C_{Π}, C_{Ψ}, C_{Ω} with their explicit expressions in (B.4) and (B.5) yields Eq. (B.7) where

$$A_{xr} = \frac{i \cdot (-2(W_w k + U_w) k^2 K_1^3 + 2W_w k^2 K_0 K_1^2 + 2W_w k^3 K_0^2 K_1)}{k^2 K_1^3 - 2k \cdot K_0 K_1^2 - k^2 K_0^2 K_1},$$
$$A_{r\theta} = \frac{i \cdot (2V_w k^2 K_1^3 + (V_w k^2 - 4V_w) k K_0 K_1^2 - 4V_w k^2 K_0^2 K_1 - V_w k^3 K_0^3)}{k^2 K_1^3 - 2k \cdot K_0 K_1^2 - k^2 K_0^2 K_1},$$
$$A_{rr} = \frac{2(-(U_w k - W_w) k^2 K_1^3 + (U_w k^3 - 2W_w \cdot k^2) K_0^2 K_1 + (U_w k - 2W_w) k K_0 K_1^2)}{k^2 K_1^3 - 2k \cdot K_0 K_1^2 - k^2 K_0^2 K_1}. \tag{B.7}$$

References

[1] S. Iijima, Nature (London) 354 (1991) 56.
[2] D. Mattia, Y. Gogotsi, Microfluid. Nanofluid. 5 (2008) 289.
[3] J.R. Freedman, D. Mattia, G. Korneva, Y. Gogotsi, G. Friedman, A.K. Fontecchio, Appl. Phys. Lett. 90 (2007) 103108.
[4] M.G. Schrlau, E.M. Falls, B.L. Ziober, H.H. Bau, Nanotechnology 19 (2008) 015101.
[5] H.J. Gao, Y. Kong, D.X. Cui, C.Z. Ozkan, Nano Lett. 3 (2003) 47.
[6] Q. Liu, B. Chen, Q.L. Wang, X.L. Shi, Z.Y. Xiao, J.X. Lin, X.H. Fang, Nano Lett. 9 (2009) 1007.
[7] D.G. Cahill, W.K. Ford, K.E. Goodson, G.D. Mahan, A. Majumdar, H.J. Maris, R. Merlin, S.R. Phillpot, J. Appl. Phys. 93 (2003) 793.
[8] G.A. Ozin, I.S. Manners, S. Fournier-Bidoz, A. Arsenault, Adv. Mater. 17 (2005) 3011.
[9] A.M. Fennimore, T.D. Yuzvinsky, W.Q. Han, M.S. Fuhrer, J. Cumings, A. Zettl, Nature 424 (2003) 408.
[10] R.M. Stevens, C.V. Nguyen, M. Meyyappan, IEEE Trans. Nanobiosci. 3 (2004) 56.
[11] J.A. Thomas, A.J.H. McGaughey, Phys. Rev. Lett. 102 (2009) 184502.
[12] C.D. Reddy, C. Lu, S. Rajendran, K.W. Liew, Appl. Phys. Lett. 90 (2007) 133122.
[13] C.D. Reddy, C.J. Lu, Appl. Phys. 103 (2008) 123509.
[14] L. Wang, Q. Ni, M. Li, Comput. Mater. Sci. 44 (2008) 821.
[15] H.L. Lee, W.J. Chang, J. Phys.: Condens. Matter 21 (2009) 115302.
[16] L. Wang, Comput. Mater. Sci. 45 (2009) 584.
[17] Y. Yan, X.Q. He, L.X. Zhang, C.M. Wang, J. Sound Vibration 319 (2009) 1003.
[18] A.M. Rao, J. Chen, E. Richter, U. Schlecht, P.C. Elund, R.C. Haddon, U.D. Venkateswaran, Phys. Rev. Lett. 86 (2001) 3895.
[19] M.S. Strano, S.K. Doorn, H. Haroz, C. Kittrell, R.H. Hauge, R.E. Smalley, Nano Lett. 3 (2003) 1091.
[20] N. Izard, D. Riehl, E. Anglarget, Phys. Rev. B 71 (2005) 195417.
[21] M.J. Longhurt, N.J. Quirke, Chem. Phys. 124 (2006) 234708.
[22] M.J. Longhurt, N.J. Quirke, Chem. Phys. 125 (2006) 184705.
[23] M.J. Longhurt, N. Quirke, Phys. Rev. Lett. 98 (2007) 145503.
[24] C.Q. Ru, Phys. Rev. B 62 (2000) 16962.
[25] F. Scarpa, S. Adhikari, J. Non-Cryst. Solids 354 (2008) 4151.
[26] F. Scarpa, S. Adhikari, J. Phys. D: Appl Phys. 41 (2008) 085306.
[27] F. Scarpa, S. Adhikari, C.Y. Wang, J. Phys. D: Appl. Phys. 42 (2009) 142002.
[28] C.Y. Wang, C.Q. Ru, A. Mioduchowski, Phys. Rev. B 72 (2005) 075414.
[29] C.Y. Wang, C.Q. Ru, A. Mioduchowski, J. Appl. Phys. 97 (2005) 024310.
[30] C.Y. Wang, C.Q. Ru, A. Mioduchowski, J. Appl. Phys. 97 (2005) 114323.
[31] C.Y. Wang, L.C. Zhang, Nanotechnology 19 (2008) 195704.
[32] C.Y. Wang, C.Q. Ru, A. Mioduchowski, Physica E 35 (2006) 48.
[33] C.Y. Wang, C.Q. Ru, A. Mioduchowski, Phys. Rev. E 74 (2006) 052901.
[34] C.Y. Wang, L.C. Zhang, J. Biomech. 41 (2008) 1892.
[35] C.Y. Wang, C.F. Li, S. Adhikari, J. Biomech. 42 (2009) 1270.
[36] J. Happel, H. Brenner, Low Reynolds Number Hydrodynamics, Noordhoff International Publishing, The Netherlands, 1973.
[37] C.E. Bottani, A.L. Bassi, M.G. Beghi, A. Podesta, P. Milani, A. Zakhidov, R. Baugham, D.A. Walters, R.E. Smalley, Phys. Rev. B 67 (2003) 155407.
[38] Y. Huang, J. Wu, K.C. Hwang, Phys. Rev. B 74 (2006) 245413.
[39] C.Y. Wang, L.C. Zhang, Nanotechnology 19 (2008) 075705.
[40] W. Flugge, Stresses in Shells, Springer-Verlag, Berlin, 1973.